The role of magnetic resonance spectroscopy in the diagnosis of brain tumors

1Maryam Sabir,2Dr Elaf Ashfaq, 3Dr Alishba Farooq, 4Momina Aslam Khan, 5Sherij Khan, 6Nisma Javed

1AIMS Hospital Muzzafarabd, maryamsabir974@gmail.com
2Women Medical Officer in Gynae & Obs Department of Amna Inayat Medical College Lahore / Kishwer Fazal Teaching Hospital Lahore.
3SKBZ CMH Mzd, farooqalishba4@gmail.com
4Medical College Muzaffarabad AJK, mominaaslamkhan@gmail.com
5PGR Neurosurgery, Mayo Hospital Lahore, sherijkhan@gmail.com
6Shaukat Khanum Cancer Hospital and Research Centre, nisma.javed90@gmail.com

ABSTRACT:

BACKGROUND: Because juvenile brain tumors may have a variety of tumor pathologies and comparable imaging appearances, noninvasive diagnosis can be difficult. when paired with conventional magnetic resonance imaging's high spatial resolution anatomical images (MRI), magnetic resonance spectroscopy (MRS) gives metabolic information from the surrounding tissue and the lesion itself. Making the distinction between malignant and non-cancerous t, as well as between low-grade and high-grade neoplasms, is crucial for selecting the best course of treatment. We used MRS to measure certain metabolic ratios and examine the metabolic profiles of various lesions in order to make a more precise diagnosis.

RESULTS: The ratios of choline to creatine (Cho/Cr), choline to N-acetyl aspartate (Cho/NAA), and choline to N-acetyl aspartate plus creatine (Cho/NAA+Crall demonstrated meaningful results at cutoffs of 0.8, 1.8, and 2, for the differentiation between neoplastic and non-neoplastic lesions. The significance of the lipid lactate peak was limited to the differentiation of high-grade from low-grade neoplasms. The metabolic profiles of choroid plexus carcinomas, medulloblastomas, and diffuse pontine gliomas were all distinctive on MRS. In comparison to high-grade neoplasms, metastasis depicted decreased Cho/NAA and Cho/Cr ratios beyond the tumor border.

CONCLUSIONS: For the non-invasive diagnosis of adolescent brain tumors, the use of important metabolic enzymes with high specificity and sensitivity to differentiate between malignant from benign tumor lesions and minimal from growing neoplasms is helpful. MRS may address sampling issues with inaccessible and different lesions as well as an unneeded sample of adenoma by evaluating tumor spatial extent and projecting tumor activity.

KEYWORDS: tumor, brain, MRS, pediatrics

DOI Number: 10.48047/NQ.2022.20.16.NQ880405 **NeuroQuantology2022;20(16):3982-3993**

INTRODUCTION: Pediatric brain tumors can be diagnosed, graded, and monitored after treatment using magnetic resonance imaging (MRI). The conventional way of MRI is the gold standard for diagnosing brain tumors, although it usually fails to accurately differentiate between high- and low-grade tumors or neoplastic from quasi-brain abnormalities [1]. Abscess, vasculitis, and other non-neoplastic brain lesions may all be mistaken for brain tumors. As a result, those with benign lesions could have unnecessary brain biopsies. Due to the range of tumor pathologies and the ambiguous or similar imaging results, it may be challenging to identify high-grade tumors from low-grade tumors. As a result, choosing the right therapy and creating the optimal treatment plan depend on having an accurate diagnosis [2].

By quantifying intracellular intermediates and investigating how they are distributed throughout the tissues, MR spectroscopy (MRS) may evaluate juvenile neurological disorders at microscopic levels. Proton spectroscopy is the MRS technique that is most extensively used. Several juvenile neurological illness processes, such as brain tumours, viral infections, anomalies in the white matter, and neonatal harm, MRS has been shown to give extra clinically useful information [3]. MRS biomarkers may supplement neuropathological data and give more insight into therapy alternatives when paired with the high-definition topographical imaging offered by conventional MRI [4]. Despite the fact that MRS is becoming more generally accessible, few research have examined how it might improve traditional radiological reporting by enhancing data gained by MRI alone [5]. In order to make a more precise diagnosis of juvenile brain tumors, this research intends to assess specific MRS metabolism fractions and metabolic profiles.

METHODOLOGY: For this research, 30 patients were prospectively included, with a mean age (SD) of 11.56 2.48 years and a range of pediatric ages of 1 to 16 years (14 male and 16 female). Between May 2020 and May 2022, they visited the pediatric oncology clinic with brain mass lesions that had been identified by CT. In accordance with the National Ethics Committee, written informed consents were acquired from the patient's guardians. All patients had thorough clinical evaluations, standard MRS and MRI tests using a 1.5T scanner equipped with the customary head coil. Numerous cases were left out of the research because of abnormalities that were too close to the full medical or nasal cavity, which produced a subpar diagnostic spectrum.

Images in the axial and sagittal planes were obtained using axial FLAIR, axial, pre-contrast T1-weighted spin-echo, and coronal T2-weighted fast spin echo. Acute axial, sagittal, and coronal differences then With Gad-DTPA (Omniscan or Magnevist) 0.1 mmol/kg, precise spin-echo pictures were taken.

At an ideal echo time (TE) of 144ms, the Point Resolved Spatial Selection (PRESS) technique was performed. The spectroscopic grid's voxels were 10 mm by 10 mm. The spectroscopic grid was manually expanded taking into consideration the lesion, any perilesional edema, and healthy brain tissue. The opposite hemisphere was examined during the MRI to the volume of interest (VOI), which revealed no anomalies. The whole scanning procedure is completed in around 5 minutes. A 35 ms additional 2D fast TE sequence was employed. The scan took roughly 12 minutes to complete.

The regions below the curve were examined and evaluated in order to find the peaking ratios (AUC). Choline (Cho) peaked at 3.2 ppm, creatine (Cr) peaked at 3 ppm, N-acetyl aspartate (NAA) peaked at 2.02 ppm, transportable triglycerides were between 0.5 and 1.5 ppm, lactate was at 1.44 ppm, and myoinositol peaked at 3.56 ppm.

Two seasoned radiologists who were not informed of the patient's clinical condition, the

results of the laboratory tests, or the demographic data examined the MRI and MRS scans. Consensus-based decisionmaking was used in every case. Stereotactic biopsy was performed in twenty-six of the thirty patients. A neuropathologist assessed each specimen histologically and in accordance with the World Health Organization (WHO) categorization. Results from MRS and histopathology were compared.

STATISTICAL ANALYSIS: The statistical analysis was carried out using statistical SPSS software. The findings were reported as standard deviations and means, whereas the descriptive analyses were provided as percentages and frequencies. Using the receiver functioning characteristic curve analysis, the connection between the spectral metabolite ratios and the pathologic results was determined. The ideal cutoff values were determined using the area under the curve for separating neoplastic from nonneoplastic lesions and limited from high-grade neoplasms (AUC). P values under 0.05 were considered to be significant. **RESULTS:** The results of 30 MRI and MRS scans revealed that 28 of them had intracranial mass lesions. In accordance with a radiological and a clinical follow-up, the remaining two individuals were identified as having acute disseminated encephalomyelitis (ADEM) in one instance and multiple sclerosis in the other. 26 of the 28 individuals with mass lesions received orthogonal biopsy and were histopathologically determined to be malignant. Two examples of brainstem gliomas were monitored clinically and radiologically but had no biopsy or surgery. The location of different lesions is shown in Table 1. Cho/Cr, Cho/NAA, and Cho/NAA+Cr all demonstrated statistically significant values for the differentiation between neoplastic and quasi lesions, with variable sensitivities and specificities, according to the ROC curve analysis (Table 2). The Cho/NAA+Cr ratio had the best specificity and sensitivity for neoplastic lesion diagnosis, scoring 88% and 100%, respectively, at a cutoff point > 0.8, with an AUC of 0.91 and a P value of 0.009.

Table 1: Final diagnostic distribution among the patients under study

Final Diagnosis Method	**30**	**%age**
ADEM	1	3.3
Multiple sclerosis	1	3.3
Brainstem glioma	2	6.7
Clinical with laboratory diagnosis	4	13.3
PNET	1	3.3
DNET	1	3.3
Recurrence of GBM	1	3.3
Metastatic lesion	1	3.3
Choroid plexus carcinoma	1	3.3
Brain abscess	2	6.7
PXA	2	6.7
Anaplastic ependymoma	2	6.7

Ependymoma	2	6.7
Medulloblastoma	2	6.7
Minimal astrocytoma	7	23.3
Superior astrocytoma	4	13.3
Histopathology	26	86.7
Total	**30**	

The Cho/NAA ratio at a cutoff point higher than 2 showed similar outcomes; it had an AUC of 0.91, a P value of 0.01, and 75% specificity and 88% sensitivity. The Cho/Cr ratio demonstrated 85% response and 75% specificity at a cutoff value of 1.86 with an AUC of 0.85 and a P value of 0.02. However, the NAA/Cr and Myo-inositol/Cr ratios did not show any statistically significant values in the prediction of neoplastic lesions with low AUC and insignificant Prob values. The ratios of Cho/NAA, Cho/Cr, Cho/NAA+Cr, and mI/Cr all showed statistically significant results for the prediction of high-grade vs. low-grade lesions, according to ROC curve analysis (Table 3). The Cho/Cr ratio had an AUC of 0.81 (P-value = 0.005) at a cutoff point > 3.5, while the Cho/NAA ratio had an AUC of 0.87 (P-value = 0.001) at a cutoff point > 3.3, according to the research. At this cutoff point, the Cho/NAA ratio exhibited a 72% specificity and a 92% sensitivity. Additionally, with AUR = 0.85 and P = 0.002, the Cho/NAA+Cr ratio showed 83% responsiveness and 72% specificity at a cutoff point of 1.3. Low-grade lesions had considerably higher myo-inositol levels.

Table 2: Analysis of the ROC curves for the different metabolite ratios

	Specificity	**Sensitivity**	***P* value**	**AUC**	**Optimal cutoff**
NAA/Cr	–	–	0.2	0.71	–
Cho/NAA+Cr	100%	88%	0.009	0.91	> 0.8
Cho/Cr	75%	85%	0.02	0.85	> 1.86
Cho/NAA	75%	88%	0.01	0.91	> 2

With an AUC of 0.9 and a P value of 0.001, the mI/Cr ratio showed 83% sensitivity and 79% specificity for the identification of increasing lesions at a threshold of 1.5. For the distinction between low-grade and high-grade neoplasms, the NAA/Cr ratio produced statistically negligible findings. A lipid lactate peak revealed that there was little specificity and sensitivity for differentiating between non-neoplastic and neoplastic lesions. Our investigation identified four distinct tumor forms in the posterior fossa: medulloblastomas, pilocytic astrocytomas, DNET, and ependymomas. Histological analysis indicated that two cases were medulloblastomas. They had higher choline levels than other posterior fossa tumors, a little increase in no lipids, lactate peaks, low NAA levels, and Myo-inositol. Cho/Cr ratios ranged from 10.6 to 14.8, with an average of 12.7 7.51; Cho/NAA ratios ranged from 22.5 to 26; Cho/NAA+Cr ratios ranged from 5.5 to 7, with an average value of 6.37 0.78; and NAA/Cho ratios ranged from 0.04 to 0.07, with a mean of 0.05 0.04; (Figs. 1 and 2).

Table 3: Metabolite ratios' ROC curve study for predicting high-grade neoplastic tumors

	Specificity	**Sensitivity**	***P* value**	**AUC**	**Optimal cutoff**
Myo-inositol (ml/Cr)	79%	83%	0.001	0.9	< 1.5
Cho/NAA+Cr	72%	83%	0.002	0.85	> 1.3
Cho/Cr	78%	83%	0.005	0.81	> 3.5
Cho/NAA	72%	92%	0.001	0.87	> 3.3

Pilocytic astrocytomas and DNET, on the other hand, revealed very slight increases in Cho peak and Cho/Cr ratio, demonstrating their lack of aggressiveness. Furthermore, NAA is found at greater concentrations compared to other tumor forms, indicating little neuronal degeneration. Four ependymoma instances were identified; two of them had grade II ependymomas that were pathologically confirmed, while the other two had grade III anaplastic ependymomas. Comparing pilocytic astrocytomas and medulloblastomas, both kinds of tumors have moderate levels of choline. The Cho/Cr ratio varied for high-grade varied between 15.8 and 25 and for low grade it was between 2.77 and 2.9, whereas the Cho/NAA ratio varied between 4.43 and 5.6 in lesser magnitude and 11.3 to 20 in high grade. In grade-II destruction of cells compared to grade III ependymomas, they were lower. In comparison to medulloblastomas or pilocytic astrocytomas, both grades of the existence of many contained more myoinositol. Both ependymomas and medulloblastomas lacked lipid-free lactate peaks, however.

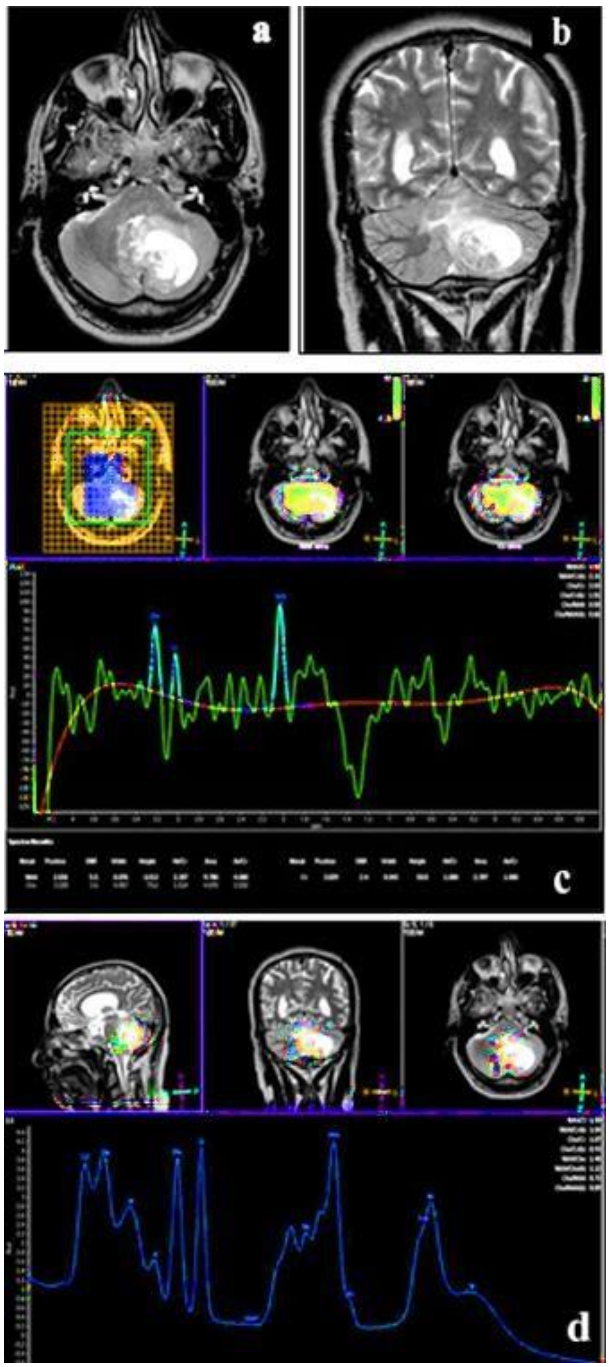

Figure 1: Different types of tumor visuals

Radiological imaging and clinical follow-up were used to find the two distributed forebrain astrocytomas in our investigation. They showed improved choline, decreased NAA, and increased creatine with Cho/Cr ratios of 2 and 1.5, 1.9 and 3, and 0.9 and 1, respectively, and increased choline, reduced NAA, and raised creatine. Lipids and lactate were not present. In this instance, choroid plexus carcinomas were discovered, which are often malignancies characterized by cellular hyperperfusion. On MRS, it had low levels of NAA, Cr, and Myo-inositol, with Cho/Cr ratios of 17, 6, and 4 and a very prominent choline peak, respectively. The

existence of a lipid/lactate peak added to the evidence of its malignant nature. Spectroscopy analysis of only one instance of rhabdomyosarcoma metastases found reduced Cho/NAA ratios (0.5) and Cho/Cr ratios (0.7). While the Cho/Cr ratio beyond the tumor margin varied from 2.4 to 3.5, with a mean of 2.53 1.38, the Cho/NAA ratio outside the tumor border in high-grade gliomas ranged from 1.7 to 7, with a mean of 3.23 2.42. Major amino acid peaking at 0.9 ppm, lactate peaking at 1.4 ppm, acetate peaking at 1.9 ppm, pyruvate/succinate not assigned peaking at 2.4 ppm with no rise in Cho, and dwarfing of other metabolites were seen in two instances of cerebral abscesses. Only this range applies to brain abscesses (Fig. 3). The case's non-conventional spectroscopic results, which included a modestly raised myo-inositol peak and mildly decreased NAA concentrations in the surrounding white matter and the lesions, led to the diagnosis of MS. The MS lesions on diffusion-weighted MRI had higher ADC values (DWI). Only one instance of ADEM with features resembling low-grade gliomas—low NAA levels, increased choline, and Myo-inositol peaks—was seen in our investigation. The occurrence of a lactate peak, however, was the defining characteristic. It displayed falling ADC readings for DWI.

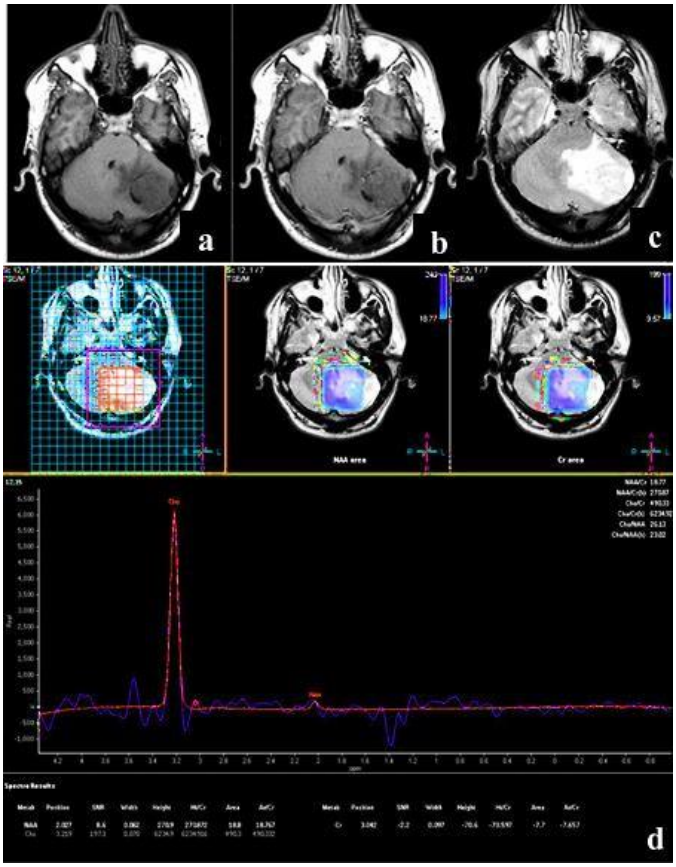

Figure 2: Different types of tumor visuals

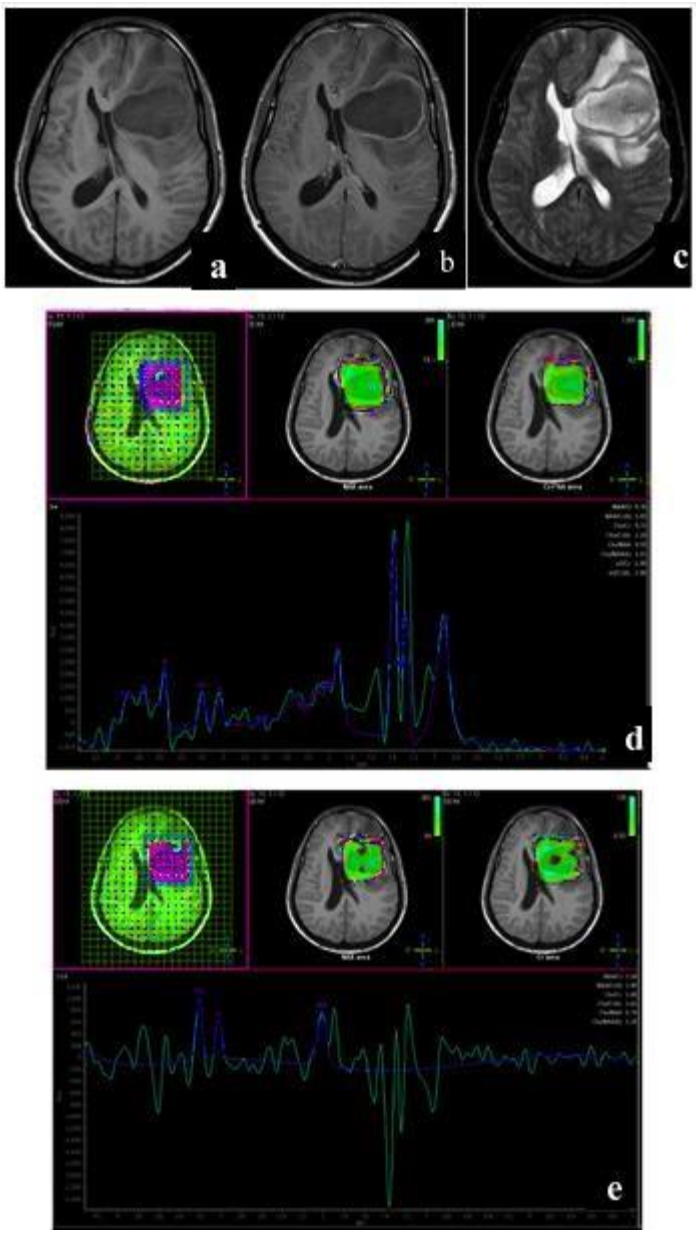

Figure 3: Different types of tumor visuals

DISCUSSIONS: The most frequent form of solid childhood cancer, the main factor that causes pediatric cancer death, and a major contributor to long-term impairment are brain tumors [6]. The gold standard for identifying juvenile brain tumors is still histopathology, but even image-guided biopsies carry a significant risk of morbidity and death. Furthermore, "sampling" inaccuracy and undegrading of the tumor are issues brought on by the heterogeneity of certain cancers [7].

In order to choose the best course of action, it is difficult to distinguish noninvasively between juvenile brain lesions that are neoplastic and those that are not, as well as between low- and high-grade neoplasms. MRS offers details on the biochemical traits, metabolic heterogeneity, and surrounding brain tissue of the lesion [8]. The capacity of distinct metabolite ratios to

identify the different brain lesions with differing sensitivity and specificity has been shown in earlier investigations. Cho/NAA, Cho/Cr, and NAA/Cho ratios were utilized in the majority of investigations, although depending only on these ratios revealed certain flaws [9]. The Cho/Naa+Cr and Myo-inositol/Cr ratios were also assessed in the present investigation to increase the diagnostic precision of MRS.

The Cho/NAA and Cho/NAA+Cr ratios in this study had the uppermost specificity and sensitivity for distinguishing between non-neoplastic and neoplastic lesions with a cutoff point of 1.86, the Cho/ Cr ratio demonstrated 85% sensitivity and 75% specificity with an AUC of 0.85 and a P value of 0.02. This study's findings were found to be consistent with a previous study [10], which confirmed that a Cho/NAA ratio > 1.83 demonstrated 100% specificity and 87.2% sensitivity for trying to distinguish between non-neoplastic and neoplastic lesions, while a Cho/Cr ratio > 1.98 demonstrated 100% specificity and 71.8% sensitivity. The cell growth index and the Cho/NAA ratio are associated with each other. [11] Additionally, they found that when a ratio is greater than 2, a neoplastic lesion can be distinguished from a non-neoplastic one with 70% specificity and 96% sensitivity. However, a lower threshold value of the Cho/NAA ratio being > 1 was used, with a sensitivity and specificity of 79% and 77%, respectively, to signal a neoplastic process. [12] However, the ratio NAA/Cr has no significant result in this research for neoplastic lesions identification with low specificity and sensitivity as well as poor AUC.

Due to the visual similarities between certain low and high-grade neoplasms, conventional MRI has a sensitivity range of 55 to 83% for assessing gliomas. The Cho/Cr ratio rises with increasing grade, NAA declines, and the lactate/lipid peak rises, according to efforts to grade tumors using MRS [13]. Additionally, another research [14] showed that the Cho/NAA ratio increased with the grade of astrocytoma.

According to the examination of the ROC curve, Cho/NAA at a cutoff point > 3.3 showed 92% sensitivity and 72% specificity for the identification of high-grade neoplasms, whereas Cho/Cr ratio at a cutoff point > 3.5 had 78% specificity and 83% sensitivity in this study. Furthermore, at a threshold of 0.5, the NAA/Cho ratio had 95% specificity and 92% sensitivity, whereas at a cutoff of >1.3, the Cho/NAA+Cr ratio showed 72% specificity and 83% sensitivity. Additional signs of a high-grade malignancy include the existence of triglycerides during MR spectral imaging and a Cho/NAA ratio greater than 2 [15].

One of the most prevalent metabolites that may be seen on MRS at short TE is Myo-inositol. The activation of protein C, contributes to the synthesis of proteolytic enzymes that are present in aggressive primary tumors [16]. In this study, the MI/Cr ratio was estimated to help with the MRS tumour grade prediction. Low-grade gliomas have substantially higher myo-inositol levels than high-grade gliomas. At a threshold value of 1.5, the MI/Cr ratio had an 83% sensitivity and a 79% specificity for identifying high-grade neoplastic lesions. This research studied the mI/Cr ratio in 20 individuals with raised gliomas, 14 patients with decreased gliomas, and 5 control cases. The results were consistent with those found in [16, 17]. In comparison to controls, Castillo found that low-grade gliomas had higher mean mI/Cr ratios (0.8 0.25), lower values for anaplastic astrocytomas (0.33 0.16), and lower values for GBM (0.15 0.12) tumours (0.4 9).

The posterior fossa is where most pediatric tumors (around 60%) start. These tumors are often ependymomas of grades II or III, grade I pilocytic astrocytomas, or grade IV medulloblastomas [3]. A posterior fossa pilocytic astrocytoma and a cystic/necrotic medulloblastoma can share comparable imaging characteristics. Furthermore, because

of their comparable appearance on conventional imaging, medulloblastoma and ependymoma are sometimes difficult to identify from one another. For the distinction of various lesions, MRS and diffusion imaging are very helpful [3].

In comparison to the other posterior fossa tumors, the two patients in this investigation with histologically proven medulloblastomas had greater choline levels, marginally higher myo-inositol levels, no lipids, lactate peaks, and lower NAA levels. Although there was no lipid or lactate peak, there were large peaks for choline and taurine that dwarfed those for other metabolites. [18] Except for the glutamate peak, which is only present in 60% of oncocytomas.

When medulloblastoma was compared to low-grade gliomas, another study discovered that the former had a three- to fourfold higher Cho level and much less NAA than the latter. [19] In their research, they also discovered that medulloblastomas exhibited lower NAA levels and lactate peaks than ependymomas, gliomas, and osteosarcoma [20]. They asserted that this metabolic profile was caused by altered glycolysis, increased membrane turnover, and decreased neuronal survival.

The Myo-inositol content of ependymomas was greater than that of medulloblastoma or pilocytic astrocytoma, however. Additionally, they exhibited levels of choline that were rather high, especially in grade III ependymomas that were in between medulloblastomas and pilocytic astrocytomas. The lactate peaks in ependymomas and medulloblastomas were devoid of lipids. Due to the heterogeneity in Cho/NAA within each tumor, it was found that ependymoma often exhibits choline elevation with reduced NAA. As a result, there is no discernible difference between medulloblastoma and ependymoma. [21,22]

Pilocytic astrocytomas in this research exhibited low levels of Cr and mI and a modestly elevated Cho and Cho/Cr ratio, This is in line with the tumor's low cell density. Furthermore, there was no lipid peak and an increased lactate doublet. Children's brain cancers consist of 10-15% diffuse pontine gliomas [23,24]. In this investigation, two instances of diffuse pontine gliomas were identified using radiology and clinical follow-up. They demonstrated increased choline and decreased NAA and creatine, indicating their neoplastic origin. Furthermore, they had no lipid or lactate peaks and somewhat low Cho/Cr and Cho/NAA ratios.

Cho level is assessed beyond the tumor border or enhancing edge to distinguish original high-grade glioma from isolated metastases. The Cho/NAA and Cho/Cr ratios evaluated outside the border of high-grade gliomas in the present research ranged from 1.7 to 7 and from 2.4 to 3.5, respectively, whereas they measured 0.5 and 0.7 in cases of metastasis.

CONCLUSION: In circumstances when a biopsy can be associated with severe morbidity, MRS improves our ability to confidently make a noninvasive diagnosis of juvenile brain tumors in clinical practice. By eliminating the biopsy of sluggish lesions and enabling early treatment planning, the use of particular metabolite proportions with high specificity and sensitivity to identify cancerous from quasi-lesion as well as low-grade from elevated neoplasms has the potential to enhance outcomes.

REFERENCES:

1. Weinberg, B. D., Kuruva, M., Shim, H., & Mullins, M. E. (2021). Clinical applications of magnetic resonance spectroscopy in brain tumors: from diagnosis to treatment. *Radiologic Clinics*, *59*(3), 349-362.
2. Ruiz-Rodado, V., Brender, J. R., Cherukuri, M. K., Gilbert, M. R., & Larion, M. (2021). Magnetic resonance spectroscopy for the study of cns malignancies. *Progress in nuclear magnetic resonance spectroscopy*, *122*, 23-41.
3. Dikaios, N. (2021). Deep learning magnetic resonance spectroscopy fingerprints of brain tumours using quantum mechanically

synthesised data. *NMR in Biomedicine*, *34*(4), e4479.

4. Galijašević, M., Steiger, R., Radović, I., Birkl-Toeglhofer, A. M., Birkl, C., Deeg, L., ... & Gizewski, E. R. (2021). Phosphorous magnetic resonance spectroscopy and molecular markers in IDH1 wild type glioblastoma. *Cancers*, *13*(14), 3569.
5. Travers, S., Joshi, K., Miller, D. C., Singh, A., Nada, A., Biedermann, G., ... & Litofsky, N. S. (2021). Reliability of Magnetic Resonance Spectroscopy and Positron Emission Tomography Computed Tomography in Differentiating Metastatic Brain Tumor Recurrence from Radiation Necrosis. *World Neurosurgery*, *151*, e1059-e1068.
6. Walchhofer, L. M., Steiger, R., Rietzler, A., Kerschbaumer, J., Freyschlag, C. F., Stockhammer, G., ... & Grams, A. E. (2021). Phosphorous magnetic resonance spectroscopy to detect regional differences of energy and membrane metabolism in naïve glioblastoma multiforme. *Cancers*, *13*(11), 2598.
7. Mui, A. W., Lee, A. W., Lee, V. H., Ng, W. T., Vardhanabhuti, V., Man, S. S., ... & Guan, X. Y.
(2021). Prognostic and therapeutic evaluation of nasopharyngeal carcinoma by dynamic contrastenhanced (DCE), diffusion-weighted (DW) magnetic resonance imaging (MRI) and magnetic resonance spectroscopy (MRS). *Magnetic Resonance Imaging*, *83*, 50-56.
8. Ji, B., Hosseini, Z., Wang, L., Zhou, L., Tu, X., & Mao, H. (2021). Spectral Wavelet-feature Analysis and Classification Assisted Denoising for enhancing magnetic resonance spectroscopy. *NMR in Biomedicine*, *34*(6), e4497.
9. Rietzler, A., Steiger, R., Mangesius, S., Walchhofer, L. M., Gothe, R. M., Schocke, M., ... & Grams, A. E. (2022). Energy metabolism measured by 31P magnetic resonance spectroscopy in the healthy human brain. *Journal of Neuroradiology*, *49*(5), 370-379.
10. Yao, R., Cheng, A., Liu, M., Zhang, Z., Jin, B., & Yu, H. (2021). The diagnostic value of apparent diffusion coefficient and proton magnetic resonance spectroscopy in the grading of pediatric gliomas. *Journal of computer assisted tomography*, *45*(2), 269.
11. Wang, Q., Zhang, J., Li, F., Chen, X., & Xu, B. (2021). The utility of magnetic resonance spectroscopy in frame-less stereotactic needle biopsy of glioma. *Journal of Clinical Neuroscience*, *88*, 102-107.
12. Morrison, M. A., & Lupo, J. M. (2021). 7-T magnetic resonance imaging in the management of brain tumors. *Magnetic Resonance Imaging Clinics*, *29*(1), 83-102.
13. Bhandari, A., Sharma, C., Ibrahim, M., Riggs, M., Jones, R., & Lasocki, A. (2021). The role of 2hydroxyglutarate magnetic resonance spectroscopy for the determination of isocitrate dehydrogenase status in lower grade gliomas versus glioblastoma: a systematic review and metaanalysis of diagnostic test accuracy. *Neuroradiology*, *63*(11), 1823-1830.
14. Maudsley, A. A., Andronesi, O. C., Barker, P. B., Bizzi, A., Bogner, W., Henning, A., ... & Soher, B. J. (2021). Advanced magnetic resonance spectroscopic neuroimaging: Experts' consensus recommendations. *NMR in Biomedicine*, *34*(5), e4309.
15. Liao, R., Zhang, D., Li, X., Ma, J., Yu, J., Yang, C., ... & Tang, Z. (2021). A preliminary study on the diagnostic efficacy of proton magnetic resonance spectroscopy at 3.0 T in rabbit with VX2 liver tumor. *Technology in Cancer Research & Treatment*, *20*, 15330338211036852.
16. Považan, M., Schär, M., Gillen, J., & Barker, P. B. (2022). Magnetic resonance spectroscopic imaging of downfield proton resonances in the human brain at 3 T.

Magnetic resonance in medicine, *87*(4), 1661-1672.

17. Dandıl, E., & Karaca, S. (2021). Detection of pseudo brain tumors via stacked LSTM neural networks using MR spectroscopy signals. *Biocybernetics and Biomedical Engineering*, *41*(1), 173195.
18. Prvulovic Bunovic, N., Sveljo, O., Kozic, D., & Boban, J. (2021). Is Elevated Choline on Magnetic Resonance Spectroscopy a Reliable Marker of Breast Lesion Malignancy?.*Frontiers in Oncology*, *11*, 610354.
19. Connelly, J. M., Prah, M. A., Santos-Pinheiro, F., Mueller, W., Cochran, E., & Schmainda, K. M. (2021). Magnetic resonance imaging mapping of brain tumor burden: clinical implications for neurosurgical management: case report. *Neurosurgery Open*, *2*(4), okab029.
20. Erchinger, V. J., Ersland, L., Aukland, S. M., Abbott, C. C., & Oltedal, L. (2021). Magnetic resonance spectroscopy in depressed subjects treated with electroconvulsive therapy—a systematic review of literature. *Frontiers in Psychiatry*, *12*, 608857.
21. Ekşi, Z., Özcan, M. E., Çakıroğlu, M., Öz, C., & Aralaşmak, A. (2021). Differentiation of multiple sclerosis lesions and low-grade brain tumors on MRS data: machine learning approaches. *Neurological Sciences*, *42*(8), 3389-3395.
22. Song, T., Song, X., Zhu, C., Patrick, R., Skurla, M., Santangelo, I., ... & Du, F. (2021). Mitochondrial dysfunction, oxidative stress, neuroinflammation, and metabolic alterations in the progression of Alzheimer's disease: A meta-analysis of in vivo magnetic resonance spectroscopy studies. *Ageing Research Reviews*, *72*, 101503.
23. Hangel, G., Lazen, P., Sharma, S., Hristoska, B., Cadrien, C., Furtner, J., ... & Trattnig, S. (2022). 7T HR FID-MRSI Compared to Amino Acid PET: Glutamine and Glycine as Promising Biomarkers in Brain Tumors. *Cancers*, *14*(9), 2163.
24. Cho, N. S., Hagiwara, A., Yao, J., Nathanson, D. A., Prins, R. M., Wang, C., ... & Ellingson, B. M. (2022). Amine-weighted chemical exchange saturation transfer magnetic resonance imaging in brain tumors. *NMR in Biomedicine*, e4785.